Heliyon 11 (2025) e42211

Contents lists available at ScienceDirect

Heliyon

journal homepage: www.cell.com/heliyon

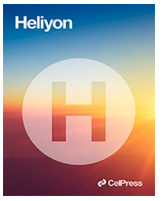

Research article

Evaluation of mechanical and thermal performance of jute and coconut fiber-reinforced epoxy composites with rice husk ash for wall insulation applications

Md. Ahtesham Akhter [a], Dipayan Mondal [a,*], Arup Kumar Debnath [a], Md. Ashraful Islam [a], Md. Sanaul Rabbi [b]

[a] Department of Mechanical Engineering, Khulna University of Engineering & Technology, Khulna-9203, Bangladesh
[b] Department of Mechanical Engineering, Chittagong University of Engineering & Technology, Chattogram-4349, Bangladesh

ARTICLE INFO

Keywords:
JF and CF with RHA
Composite specimens
Tensile and flexural properties
Thermal properties
Heat transfer
Wall insulation

ABSTRACT

This study aimed to investigate the mechanical properties and thermal properties of epoxy composites reinforced jute and coconut fibers with varied rice husk ash (RHA) percentages for thermal insulation in building wall insulation. In this study, according to ASTM standards, the seven types of composite samples with varying filler ratios were prepared using the hand lay-up process. The four jute fiber (JF) samples were prepared with RHA at 0 % (control), 1 %, 2 %, and 3 % of total weight respectively, while the other three coconut fiber (CF) samples were prepared with CF at 0 % (control), 1 %, and 3 % RHA, respectively. The mechanical and thermal properties were measured for repeated three samples by using the UTM and TRSYS101 units, respectively. Regarding the mechanical characteristics, tensile strength increased with the increment of filler percentage for jute fiber composites, however, tensile strength reduced in the coconut coir composites as the filler percentage increased. The jute fiber composite sample consisting of 3 % RHA was found to be the highest among the seven composite samples, with a maximum ultimate tensile strength of 50.07 MPa and the highest tensile modulus of elasticity (2.85 GPa) with better energy absorption property. In terms of flexural strength tests, with the increase of filler percentage in coconut coir composites, the flexural properties decreased as well. On the contrary for jute fiber composites, 3 % RHA-JF composite had the highest flexural strength and moderate flexural modulus of elasticity. This study also found that with the increase of RHA percentage in JF composites, the thermal conductivity decreases, with a minimum value of 0.03697 W/m.K was found in 3 % RHA-JF composite, while in CF composites, it increased with the filler percentage. However, the combined uncertainties of mechanical properties (tensile and flexural) are estimated at 4.57 % and 4.93 %, respectively, while estimated at 5.67 % for thermal conductivity measurement. As, 3 % RHA-JF composite offers low thermal conductivity, good strength, and energy absorption, it is suitable for thermal insulation applications. Furthermore, the heat transfer analysis has been studied analytically by considering two types of wall insulation configurations (type 1 and type 2). Due to its easy capability to insert or attach inside the wall insulation and get almost similar heat transfer rate, type 2 is considered in actual practice of wall

* Corresponding author.
E-mail address: dipkuet@me.kuet.ac.bd (D. Mondal).

https://doi.org/10.1016/j.heliyon.2025.e42211
Received 10 October 2024; Received in revised form 21 January 2025; Accepted 21 January 2025
Available online 23 January 2025

insulation. Moreover, the scope of this study is to explore agricultural waste to reduce environmental impact and enhance energy efficiency through thermal insulation inserted inside the domestic building's wall.

Nomenclature

A	the cross-sectional area through which heat is flowing (m^2)	q	average heat flux (W/m^2)
b	width of test beam (mm)	Q	heat transfer through the wall (W)
d	depth or thickness of the tested beam (mm)	R	radius of the beam (mm)
D	maximum deflection of the center of the beam (mm)	T_1	outer surface temperature of the composite wall (°C)
dT	temperature difference (°C)	T_4	the inner surface temperature of the composite wall (°C)
dx	sample thickness (m)	x_8, x_9, x_{10}	thickness of concrete layer in the composite wall (mm)
E_f	flexural modulus of elasticity (MPa)	x_i	thickness of the insulating material (mm)
E_t	tensile modulus (MPa)	*Greek characters*	
F	applied force (N)	σ_t	tensile Stress (MPa)
$Fmax$	maximum force applied before failure (N)	ϵ_t	tensile strain (dimensionless, often expressed as a percentage)
k_i	thermal conductivity of the insulating materials (W/m.K)	σ_f	modulus of rupture, stress required to fracture the sample (MPa)
k_8, k_9, k_{10}	thermal conductivity of the concrete layer (W/m.K)	ϵ_f	strain in the outer surface (mm/mm)
L_0	original length of specimen (m)		*Subscripts*
L	final length of the specimen (m)	i	1, 2 … … … 6
m	gradient of the straight-line portion of the load-deflection curve (N/mm)	max	maximum

1. Introduction

Thermal comfort significantly influences daily activities, especially in tropical regions where heat waves can elevate indoor temperatures, thereby impacting human work performance. Warm temperatures inside the structure must be tolerated without compromising building strength. Buildings lose heat through infiltration and exterior walls, ceilings, windows, and basements. A well-designed building insulation system that acts as a heat transfer barrier is necessary to achieve thermal comfort. Insulation keeps rooms cool in summer and warm in winter, creating a comfortable environment for daily activities [1]. Typically, insulation-related materials are put between internal and exterior walls in attic floors or ceilings. Storm doors and windows improve insulation by producing dead gaps and weather-stripping frames. The need for inexpensive, lightweight, and structurally sound insulating materials has grown as a result of standard engineering materials' high strength, low density, and low conductivity. A common material for thermal insulation is foamed plastic, however, its mechanical characteristics restrict its use [2]. In these circumstances, composite materials may be used as an alternative. These materials consist of at least two independent phases or combinations of phases connected at the interface, each originating from different elemental materials [1]. Synthetic fibers like glass fiber, nylon fiber, and carbon fiber are potential fiber materials for structure and wear-resistant components. Their low density and exceptional specific stiffness made them valuable engineering materials. Glass fiber-reinforced polymer matrix composites enhance insulating capability. However, they are non-recyclable, costly, and have caustic and poisonous properties [2]. Natural fibers like jute, coconut coir, rice husk, and banana can be used to their full potential, while polymer materials are versatile and can be modified with fillers, fibers, and additives. Research is enhancing natural fiber-reinforced polymer composites (NFRPC), which are increasingly utilized in various industries due to their low cost, ecological benefits, and mechanical properties. NFRPCs, made from fibers like jute, sisal, bamboo, and coconut coir, offer advantages such as being lightweight, nontoxic, biodegradable, and effective insulators. Their non-abrasive nature and carbon-absorbing capacity make them appealing alternatives to synthetic fibers, particularly in automotive applications [3,4] The development of lightweight, porous materials aims to further improve their mechanical strength and thermal insulation [2]. Composites have been used since 1500 BC, with modern fiber-reinforced versions emerging in 1945 for military use. Composites are classified into types based on reinforcement: particle-reinforced, fiber-reinforced, and structural. They can also be categorized by matrix, which binds the reinforcing material. Polymer matrix composites use fibers in organic polymers to enhance properties, offering low weight, corrosion resistance, and excellent insulation [5,6,7]. Metal matrix composites (MMC) consist of a metal combined with another material, while ceramic matrix composites (CMC) are high-temperature, non-metallic materials with ceramic fibers, known for corrosion and thermal resistance [8,9,10]. Natural fiber-reinforced composites are lightweight, cost-effective, and eco-friendly but face challenges like moisture resistance. However, incompatibility and low moisture resistance hinder their development [11,12]. In contrast, synthetic fibers like nylon and polyester are used in fiberglass but are less favored due to high cost and non-biodegradability [13].

Zakriya and Ramakrishnan [14] studied the insulation and mechanical properties of jute and hollow-conjugated polyester-reinforced nonwoven composites, finding superior qualities such as tensile strength, Young's modulus, hardness, and impact strength. Praveena et al. [15] examined the mechanical, thermal, machinability, and biodegradability properties of natural fiber-reinforced polymer composites, emphasizing their environmental benefits and potential applications in interior housing, automobiles, marine, and residential sectors. Sarukasan et al. [16] created a jute-coir hybrid composite using compression molding, with the length of 20 mm fibers providing the highest tensile strength and flexural strength. Florea and Manea [17] found that only two recipes: sheep wool and gypsum, hemp fibers and gypsum met the required standards for thermal conductivity, offering low rigidity,

heat conductivity, low health impact, energy efficiency, ease of use, and environmental performance. Ghazi and Jaddan [18] studied the thermal conductivity of epoxy-based composites reinforced with date palm waste particles, aiming to create green materials for shipbuilding and vehicles. Jani et al. [19] explored the mechanical and thermal insulation properties of surface-modified Agave Americana/carbon fiber hybrid epoxy composites, using a Universal Testing Machine (UTM) to test mechanical properties. Boopalan et al. [20] analyzed the mechanical and thermal characteristics of jute and banana fiber-reinforced epoxy hybrid composites, finding that adding up to 50 % banana fiber increased the composites' characteristics while minimizing moisture absorption. Bhoopathi et al. [21] developed and assessed banana, hemp, and glass fiber composites for tensile, flexural, and impact strength. Hybrid composites reinforced with natural and synthetic fibers with varying percentages of fillers have higher elastic moduli and better energy dissipation [22]. Jahir et al. [23] researched jute and glass fiber-reinforced epoxy composite to strengthen the natural fiber. They examined how synthetic fiber orientation affected the composite's mechanical characteristics. Additionally, carbon fiber and glass fiber were used by Debnath et al. [24] as a reinforcing element with the timber beams to boost their strength.

Research on hybrid composites with carbon-Kevlar-basalt-innegra fibers and fillers optimized mechanical and thermal properties through artificial neural network (ANN) modeling [25]. Adding titanium carbide nanofillers and coir microparticles improved the mechanical and thermal stability of basalt-innegra fiber composites. Biowaste fillers like banana, pineapple, and coir fly ash enhanced hybrid fiber epoxy composites [26]. Natural fiber-reinforced laminates outperformed glass fiber composites, with fibers placed at a 45-degree angle showing superior properties [27]. Banana fiber composites exhibited better wear performance and lower density than glass fiber composites. Treated banana-coir fiber epoxy composites had higher tensile and impact strengths, while untreated fibers had higher flexural strength. Coconut shell fillers in hybrid fiber composites improved tensile, flexural, and impact strengths and reduced wear-induced weight loss [28]. Sankar et al. [29] employed polypropylene and banana fiber to make hydrophobically treated composite specimens, showing significant tensile and flexural strength, demonstrating the potential of natural fiber-reinforced plastics to minimize carbon footprints and encourage industries to switch to fiber-reinforced polymers (FRP). Moreover, Hameed et al. [30] researched the effect of rice husk and ash on coconut fiber-reinforced polyester composites, finding that flexural strength rose with fiber content but hardness increased with coconut fiber content. Combining natural and synthetic fibers with fillers improved elastic modulus and energy dissipation [31]. Nano filler-added glass/epoxy composites showed better mechanical behavior, and functionalized graphene improved the properties of glass fiber epoxy nanocomposites [32]. Chen [33] research on insulating walls using natural fiber bio-composites revealed increased flexural strength, compressive strength, and elastic modulus with increasing wood fiber content. The bio-composites were excellent for wall insulation because of their good thermal insulation capacity and thermal conductivity, which ranged from 0.078 to 0.089 W/(m. K). Tutur et al. [34] introduced the replacement of ordinary Portland cement with coconut fiber combined with rice husk ash as a potential that could interact between the fibers and the matrix and also influence the overall performance of the composite, while Hameed et al. [30] incorporated RHA that may adversely affect the hardness properties of the composite, possibly due to the interactions between the fiber and the filler material. Omar et al. [35] explored the potential of using coconut fiber with fire retardant paint as a thermal comfort for building ceiling boards. A low-temperature quality of 0.225 W was found and suggested the fiber is ideal as an insulating material. Hasan et al. [36] developed insulating panels using long and short coconut fiber and investigated the thermal properties. It is reported that the thermal conductivity was measured within 0.046280–0.062400 W/m.K of the composites, suggesting superior insulating properties. Veeraprabahar et al. [37] prepared the hybrid composite for various loadings of coconut/jute fiber and conducted the thermal insulation characterization. The results showed that the porous composites possess excellent performance in thermal insulation of high-temperature heat waves, especially above 350 °C. Building walls significantly enhance energy efficiency and thermal comfort by minimizing heat transfer. Investing in high-quality, well-designed walls is crucial for optimizing energy consumption and occupant comfort. Composite walls, made up of two bonded components, offer superior insulation and control over heat flow, making them lightweight, affordable, and better suited for thermal comfort [38]. In addition, Ahmad et al. [39] reported a review of Zr-based metal-organic frameworks (MOFs) whose targets were the study of stability and the factors affecting the stability of Zr-MOFs, including the adsorbent capacities, kinetics, and thermodynamics. Meanwhile, Naseem et al. [40] introduced a review of the smart polymer based on the enzyme encapsulation system which enhances the lifetime and tunes the biomedical activities.

Numerous studies have been conducted to explore the methods for enhancing the mechanical strength of epoxy-based composite materials by incorporating various fillers. While these efforts have yielded significant advancements, a notable gap remains in understanding the combined impact of natural fibers and agricultural byproducts, such as rice husk ash, as fillers. There is little to no research on the combined impact of natural fibers and rice husk ash composites for being used in building wall insulation. Despite the growing interest in sustainable and efficient thermal insulation materials, the synergistic effects of natural fibers and rice husk ash in epoxy composites have not been extensively studied. Additionally, there is a lack of comprehensive research investigating the optimal use of rice husk ash as a filler, particularly regarding how varying filler ratios influence the thermal and mechanical properties of these composites. However, this research generated seven composite samples (0–3 % RHA with jute and coconut fibers): four of jute fiber and three of coconut fiber with varying rice husk ash content. Thermal and mechanical tests were performed on the samples, and the optimal filler and fiber combination was determined by comparing composites with varying filler percentages. A heat transfer analysis was also done for the composite samples. By using the measured thermal conductivity of the composites, the heat transfer rate was calculated for two different types of walls. Consequently, the goal of this research was to evaluate the impacts of applying various dosages of rice husk ash to provide thermal insulation and to investigate the effects of this filler on the mechanical and thermal characteristics of epoxy composites reinforced with jute and coconut fiber.

2. Methodology and experimental apparatus

2.1. Material selection

In this work, two types of fibers (jute and coconut) are used due to the high silica content, and rice husk ash (RHA) is used in varying proportions as a cost-effective and easily available filler material for natural fiber-reinforced epoxy composites. Moreover, as per Ch et al. [41], RHA enhances mechanical properties like impact resistance, tensile strength, and flexural strength and also improves thermal characteristics by serving as an insulating barrier, making it suitable for energy-efficient building insulation. Epoxy resin is more favorable than any other polymer matrix due to its chemical resistance, high-temperature resistance, toughness, minimal drying shrinkage, and corrosion resistance. A hardener is used with resin as a binder named triethylenetetramine and a releasing agent, specifically wax is used for seeking for easy removal of the prepared specimens from the mold. LS800 grade 3:1 ratio epoxy hardener is used for this study. The properties of LS800 grade epoxy are listed in Table 1, and the properties of JF, CF, and RHA are listed in Table 2. At first, the rice husk was cleaned to eliminate contaminants before being screened for filth. To make the ash used in this study, rice husk was air-dried for 48 h and burned for about 6 h at 550 °C in a furnace [42]. While, the wax is used as a releasing agent in composite manufacturing to ensure the smooth removal of composite plates from mold, prevent adhesion, and shield the mold surface from resins and abrasive materials.

2.2. Fabrication of specimen

Fig. 1 shows the schematic diagram of the fabrication process for composite samples. By the way, the composite fabrication process involved using glass plates with a 300 × 300 × 20 mm^3 mold size for uniform layer formation. Fiber mats were cut into the same shape based on the mold size, using masking tape and permanent markers to prevent edge damage. RHA filler mixed with epoxy resin (3:1 ratio of resin and hardener) through sonication for uniform distribution. The process was completed using a digital weight balance for accurate weight measurements. The specimen was prepared using the hand lay-up process [50], which involves placing transparent polythene on a mold, attaching it with masking tape, and evenly dispersing a resin-hardener mixture across it. At first, the mixture of epoxy resin and RHA was prepared to pour into the mold with the fiber mat. The fiber mat was then positioned and burnished using epoxy, ensuring all fibers were saturated with epoxy and no dry areas. When all the layers were soaked with resin, the composite was wrapped in polythene to prevent air from entering and preventing a void fraction. After that, the prepared sample is pressurized by a smooth weight block for a certain time to ensure uniform thickness until the solidification occurs under the weight block into the mold. Then, the prepared sample is to be cleaned and cut into the specific standards, and the test samples as in section 2.3.

2.3. Experimental apparatus

2.3.1. Tensile test

The tensile strength, strain, modulus, and ultimate tensile strength are key mechanical properties evaluated in materials. A tensile test was conducted on a composite material with three samples for each specimen by using ASTM D3039 [51]. The test involved axially loading the specimen clamped in the jaws of a Shimadzu AGX-V 300 KN UTM machine [52]. The gauge length was set based on the ASTM standard and maintained at 91 mm in all the samples. Under 2 mm/min loading, the fiber and matrix bonded until fracture occurred at the ultimate breaking load. Rectangular specimens (200 mm × 25 mm) were cut from the composite plate as per ASTM D3909. In a tensile test using a UTM for a composite sample, several key equations are used to describe the mechanical properties of the composite samples. The primary equations and the parameters [53] for measuring the tensile strength, tensile strain, tensile modulus, and ultimate tensile strength are listed as follows from Eqs. (1)–(4), respectively:

$$\sigma_t = \frac{F}{A} \tag{1}$$

$$\varepsilon_t = \frac{L - L_0}{L_0} \tag{2}$$

$$E_t = \frac{\sigma_t}{\varepsilon_t} \tag{3}$$

Table 1
Properties of LS800 grade epoxy [43].

Part	800A	800B
Color	Transparent	Transparent
Specific Gravity	1.15	0.97
Viscosity (25 °C)	2000-4000CPS	50MAXCPS
Mixing Ratio	A: B = 100:33(weight ratio)	
Hardening Conditions	25 °C × 24H–48H (100g)	
Useable Time	25 °C × 120min (100g)	

Table 2
Properties of jute fiber (JF), coconut fiber (CF), and rice husk ash (RHA).

Properties	JF [44,45]	CF [45,46]	RHA [47,48,49]
Tensile strength, MPa	300–1200	40–90	–
Moisture content, %	12–14	10–15	2.15
Fiber length, cm	1–4	10–30	–
Density, g/cm^3	1.3	1.15	0.495
pH	6.5–7.5	5.5–6.8	–
Thermal conductivity, W/mK	0.035–0.042	0.05–0.1	–
Water retention capacity, %	200–400	400–500	–
Chemical composition	Cellulose (60–70 %), Hemicellulose (10–15 %), Lignin (10–15 %), Pectin (1–2%)	Cellulose (43–45 %), Lignin (22–33 %), Hemicellulose (19–26 %), Pectin (1–3%)	SiO_2 (80.7–95.87 %), Al_2O_3 (0.36–0.41 %), Fe_2O_3 (0.13–2.86 %), CaO (1.12–1.5 %), MgO (0.30–0.82 %), SO_3 (0.67–1.17 %), Na_2O (0.85–1.15 %), K_2O (0.77–2.11 %), LOI (2.81–6.55 %)
Color	Off-white to brown	Light brown to golden brown	Grey
Specific gravity	1.30–1.48	1.34–1.98	2.02–2.21

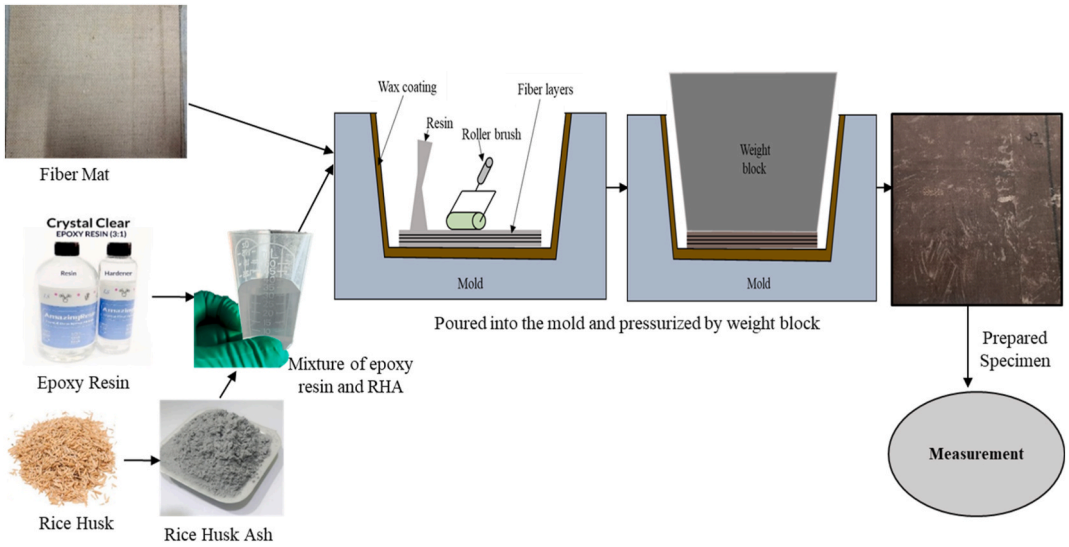

Fig. 1. Schematic diagram of the fabrication process for composite samples.

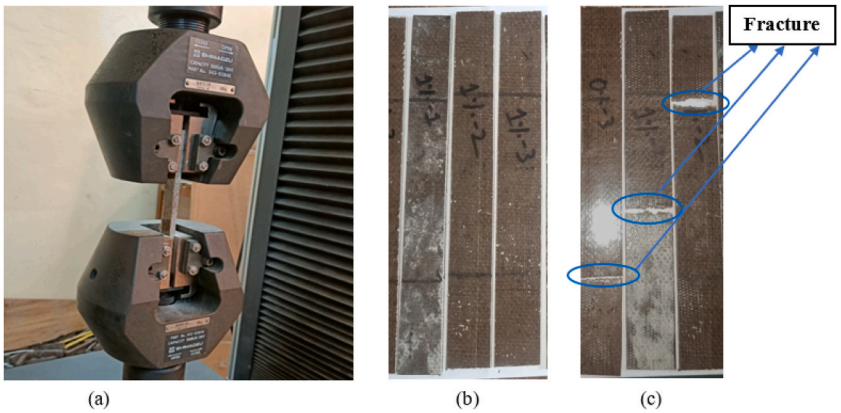

Fig. 2. Tensile test: (a) specimen at UTM, (b) specimen before the test, and (c) specimen after the test.

$$UTS = \frac{F_{max}}{A} \tag{4}$$

where σ_t is the tensile strength (MPa), ϵ_t is the tensile strain (as a percentage), and E_t is the tensile modulus (MPa), respectively. A force F is applied to the specimen to measure the tensile test. Where F is applied force (N), A is the original cross-sectional area of the specimen (m^2), L_0 is the original length of the specimen (m), L is the final length of the specimen (m) and $Fmax$ is the maximum force applied before failure (N). Fig. 2(a–c) illustrates the specimen at UTM, the specimen before the test, and the specimen after the test, respectively. The noticeable fracture of the specimen was found after the test, and the obtained results are presented in section 3.1.

2.3.2. Flexural test

For the flexural test, the specimens were prepared according to the ASTM D790 [54] standards and examined three samples for each specimen. In this study, the 3-point test was considered which is the most common flexural test and also known as the three-point bending method for prepared composite samples. The test was carried out in the UTM, while the flexural test specimen size was specified to be in the form of a rectangle in ASTM D790 [54]. Initially, a rectangular specimen was cut from the fabricated composite plate using a circular saw machine according to thickness. The span length of each specimen of jute fiber was 68 mm and each specimen of coconut fiber was 119.5 mm long as per ASTM 790 standard and at a cross head speed of 5 mm/min of stroke was used to test all specimens. Fig. 3 shows the universal testing machine for flexural test measurement, while Fig. 3(a) shows the specimen at UTM, and Fig. 3 (b) and (c) interpret the specimen before the test and the specimen after the test, respectively. A noticeable fracture of the specimen was found after the test and the obtained test results are incorporated in the result and discussion section in 3.2.

In a three-point flexural test of composite materials using a UTM, the primary equations [55] used to determine the flexural strength (σ_f), flexural modulus (E_f), and strain (ϵ_f) are listed in Eq. (5), Eq. (6), and Eq. (7), respectively, as follows:

$$\sigma_f = \frac{3FL}{2bd^2} \tag{5}$$

$$E_f = \frac{L^3 m}{4bd^3} \tag{6}$$

$$\varepsilon_f = \frac{6Dd}{L^2} \tag{7}$$

where σ_f is the modulus of rupture, the stress required to fracture the sample (MPa), ϵ_f is the strain in the outer surface (mm/mm), E_f is the flexural modulus of elasticity (MPa), F is the load at a given point on the load-deflection curve (N), L is the support span (mm), b is the width of test beam (mm), d is the depth or thickness of tested beam (mm), D is the maximum deflection of the center of the beam (mm), m is the gradient of the initial straight-line portion of the load-deflection curve (N/mm), and R is the radius of the beam (mm).

2.3.3. Thermal test

Fig. 4 shows the thermal conductivity measuring apparatus which consists of a TRSYS01 unit with a data logger, temperature sensor, heat flux sensor, heater, measurement chamber, and insulator. It measures thermal transmittance and resistance, following ASTM C1155/C1046 and ISO 9869 standards. The system includes two heat flux sensors, matching thermocouples, and high-accuracy electronics. The system provides high confidence in results due to redundancy at two locations, and its accuracy ensures continuous monitoring even when other systems fail. The HFP01 sensor measures heat flux through walls, building envelopes, and soil [56]. However, the composite was set up into a rectangular shape frame with dimensions of 147.30 × 203.20 × 10 mm. The data logger was attached to the outer surface of the sample and placed in contact with a heat source inside the chamber. A temperature sensor was attached to the opposite surface of the sample. A heat flux sensor was also attached to the outer surface. The heat source was turned on and, it was allowed to reach a steady temperature. Temperature readings were recorded in the data logger from the temperature sensor

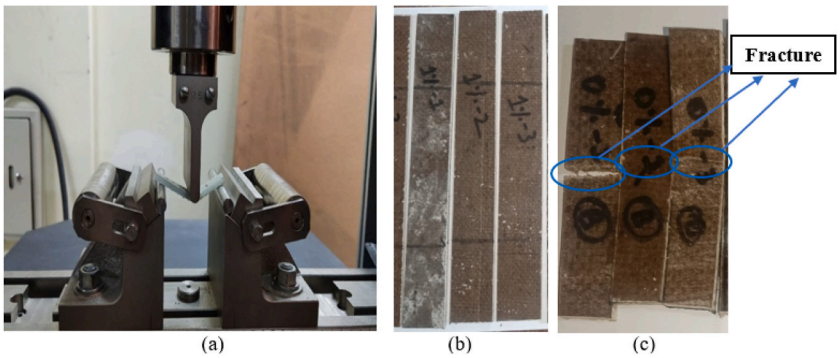

Fig. 3. Flexural test: (a) specimen at UTM, (b) specimen before the test, and (c) specimen after the test.

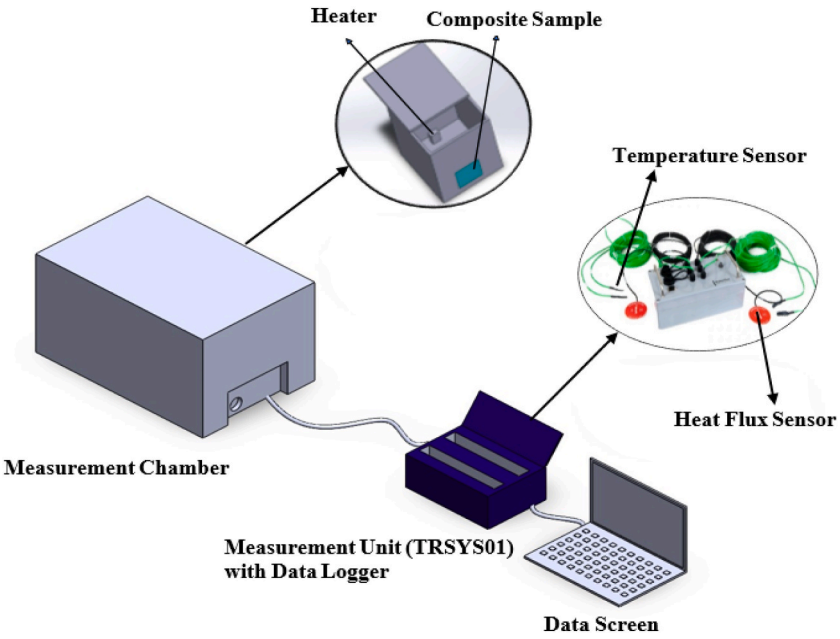

Fig. 4. Experimental setup for measuring the thermal conductivity of prepared composites.

at regular intervals. The heat flux was calculated from the power input to the heat source, and the temperature difference was determined from the difference between the readings from the data logger and the temperature sensor. The thermal conductivity of the sample was calculated using Eq. (8) of Fourier's law of heat conduction [57] as follows:

$$k = \frac{q \times dx}{dT} \tag{8}$$

where k is the thermal conductivity, q is the heat flux, dT is the temperature difference, and dx is the thickness of the sample. The measurement was repeated several times in order to get the average heat flux and temperature difference. Each data was taken at every 10 min interval and the total measurement period was around 5–7 h.

2.4. Apparatus reliability

The Shimadzu AGX-V 300 KN UTM was utilized for both tensile and flexural properties, and the TRSYS01 unit was used to measure the thermal properties in this study. To ensure the reliability of the apparatus, the variability in the test results was compared with previous studies that used the same equipment. For tensile tests, Karua et al. [58] reported a compressive strength of 3.15 ± 0.17 MPa for jute fiber reinforced with perlite and a flexural strength of 1.96 ± 0.35 MPa for the same sample. Saif and Islam [59] recorded a tensile strength of 31.84 ± 1.07 MPa for untreated bagasse fiber, with a standard deviation of 1.07 MPa across five samples. In comparison, the standard deviation (SD) for the tensile strength in this study was 1.28 MPa for the jute fiber-reinforced (JF) epoxy composite with 1 % RHA, 2.03 MPa for 0 % RHA, and 1.28 MPa for 3 % RHA. For flexural tests, Karua et al. [58] reported an SD of 0.35 MPa, while Hossain et al. [60] observed a range from 0.40 MPa to 2.95 MPa for different sandwich structures. In this study, the standard deviation for flexural strength was 1.146 MPa for 0 % RHA and 1.9614 MPa for 1 % RHA composites. Although some values in this study exhibit greater variability than those reported by Karua et al. [58] and Saif and Islam [59], this is largely due to differences in fiber treatment and composite preparation processes, as well as the complex interactions between jute fibers and RHA in the epoxy matrix. To further assess reliability, the coefficient of variation (CV) was calculated. Saif and Islam [59] reported a CV of 3.36 % for untreated bagasse fiber in tensile strength, and Karua et al. [58] calculated a CV of 17.86 % for flexural strength. The CV values for the tensile strength in our study were higher, reflecting the unique characteristics of the RHA-jute fiber composites under evaluation. Despite the observed variability, the repeatability of the testing procedures and consistent loading rates affirm the precision of the Shimadzu AGX-V 300 KN across varying material systems. Additionally, the TRSYS01 heat flux measuring system was used to evaluate thermal performance. Hossain [61] reported an uncertainty percentage of ±6 % for roof material and ±4.95 % for wall material when using this device. Hence, the consistent test parameters, such as the loading rate of 5 mm/min in both this study and the comparison studies, demonstrate that the Shimadzu AGX-V 300 KN provides reliable results under different material and testing conditions. Given the consistency in measurement and the known uncertainty levels, the reliability of the thermal performance data in this study is well within acceptable bounds for experimental apparatus.

2.5. Uncertainty measurement

The uncertainties of these measurements were estimated by the GUM (Guide to the Expression of Uncertainty in Measurement) guideline using the law of propagation [62,63,64]. The accuracy of these measurements was influenced by several important parameters introduced during the measurements. The most common input variables that cause uncertainty in the tensile test are the invariability in the thickness of the specimens, variation in gauge length, and variation in the orientation of the sample. Change in loading rate can also be a major factor while evaluating tensile strength. For flexural tests, span length, specimen thickness, and fiber orientation are the key factors for the uncertainty. Loading rate plays an important role in this part as well [65,66]. Moreover, the thermal conductivity measurement includes inaccuracy owing to the hot and cold surface temperature of the tested walls and roofs as well as heat flux. In addition, the uncertainty estimation varies from the test specimen dimension, measurement condition, also the obtained parameter measurement, and so on.

However, the combined standard uncertainty $u_c(Y)$ is the positive square root of the combined variance $u_c^2(Y)$, generally written as below as Eq. (9) which is utilized and followed by several researchers [65,66,67,68,69,70].

$$u_c^2(Y) = \sum_{i=1}^{N} \left[\left(\frac{\partial Y(X)}{\partial X_i} \right)^2 . \; u^2(X_i) \right] \tag{9}$$

where $u^2(X_i)$ are the variances of several input parameters X_i,i $= 1,2,3,.....$N. The standard uncertainty $u(X_i)$ is defined as type-A and/or type-B, depending on whether it is random or systematic, where type-A means random consideration and type-B is systematic consideration. The type-A evaluation comes from the measurement errors, whereas the type-B evaluation is from the reading instrument or calibration. Finally, the combined uncertainties of mechanical properties (tensile and flexural) are estimated at 4.57 % and 4.93 %, respectively, while estimated at 5.67 % for thermal conductivity measurement.

3. Results and discussion

3.1. Tensile properties

The tensile test results are listed in Table 3, while the stress vs. strain curve and the force vs. displacement curve are presented later based on the obtained data.

Fig. 5 presents the tensile stress vs. strain curve, where the stresses are increased with the strain at the maximum amount for seven specimens. The maximum stress value for the 3 % RHA + JF sample (51.04 MPa) is the highest of them. This is followed by the 2 % RHA + JF sample (50.87 MPa), the 1 % RHA + JF sample (42.92 MPa), the 0 % RHA + JF sample (36.51 MPa), while the 0 % RHA + CF sample (20.35 MPa), 1 % RHA + CF sample (19.53 MPa), and lastly the 3 % RHA + CF sample (15.61 MPa) that has the lowest value of tensile stress. Compared to other composites, the strain value for the composite sample consisting of 3 % RHA and jute fiber is fairly good. This suggests that the composite made of 3 % RHA and jute fiber has moderate ductility. Among the seven samples, the 3 % RHA + Jute Fiber composite had the highest strength and highest degree of ductility, making it an excellent choice for structural applications requiring both strength and flexibility. As per the study by De Silva and Naveen [71], with the increase of RHA percentage with coconut fiber, workability decreases. In this study, we have observed less strength for the 3 % RHA + CF compared to 1 %, and 0 %

Table 3
Tensile test results.

SL	Specimen Name	Ultimate Force (N)	Tensile Modulus of Elasticity (GPa)	Ultimate Tensile Strength (MPa)	Energy Absorption (J)
1	0 % RHA + JF	3571.71	2.323	32.8694	8.2985
		4182.85	2.249	36.2205	10.5237
		4367.154	1.992	36.5188	11.1151
2	1 % RHA + JF	5057.673	2.495	42.5454	14.0182
		4835.148	2.07	40.5338	12.6777
		4839.3	1.815	42.9230	14.1727
3	2 % RHA + JF	5501.101	2.600	50.8777	18.2207
		5414.976	2.046	48.4863	20.4366
		5492.234	2.146	50.2947	19.0252
4	3 % RHA + JF	5580.222	3.046	50.5433	15.6575
		5271.090	2.678	48.6206	17.4798
		5550.697	2.839	51.0412	15.3270
5	0 % RHA + CF	3801	1.624	20.3597	5.7611
		3516	1.253	18.0470	5.3407
		3836	1.616	20.1949	5.7621
6	1 % RHA + CF	3589.74	1.432	18.4897	6.0581
		3368.85	1.405	16.7653	6.1539
		3289.95	1.344	19.5323	5.9896
7	3 % RHA + CF	2832.57	1.225	14.4640	6.8008
		2780.448	0.975	14.4321	6.8969
		2884.476	0.996	15.6154	7.4691

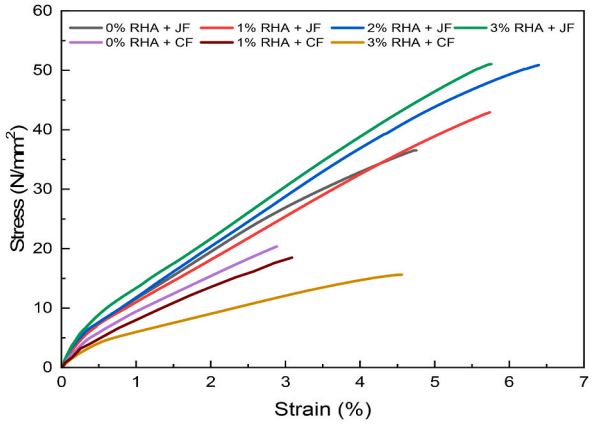

Fig. 5. Tensile test stress vs. strain curve.

RHA with CF.

Fig. 6 indicates the tensile force vs. displacement curve, where the force would be sustained at a maximum amount with the displacement, and after that, the rapture/fracture occurred at maximum displacement. It is found that the 3 % RHA and jute fiber composite sample performs significantly better than the other samples, with a maximum force of 5580.22 N. With 5501.10 N, the composite sample consisting of 2 % RHA and jute fiber has the second-highest maximum force value. The maximum forces of the composites with 1 % RHA + JF, 0 % RHA + JF, 0 % RHA + CF, 1 % RHA + CF, and 3 % RHA + CF are 5057.673 N, 4367.154 N, 3836 N, 3589.74 N, and 2884.476 N, respectively.

Based on the bar chart data shown in Fig. 7, it is clear that the seven different composite samples have significantly different tensile properties. In terms of ultimate tensile strength, the 3 % RHA + JF composite has the highest value for average tensile strength of 50.07 MPa, followed by the 2 % RHA + JF sample (49.89 MPa), the 1 % RHA + JF sample (42.00 MPa), the 0 % RHA + JF sample (35.20 MPa), the 0 % RHA + CF sample (19.53 MPa), the 1 % RHA + CF sample (18.26 MPa), and lastly the 3 % RHA + CF sample (14.87 MPa) that has the lower value of ultimate tensile strength. In terms of stiffness, the 3 % RHA and jute fiber composite also have the highest tensile modulus of elasticity (avg.) of 2.85 GPa. This indicates that the 3 % RHA + JF composite is the stiffest material of the seven, while the 3 % RHA + CF composite is the most flexible. The other composites appear to be an intermediate between the 3 % RHA + CF and 3 % RHA + JF composites in terms of both strength and stiffness.

3.2. *Flexural properties*

The flexural test results are listed in Table 4, while the stress vs. strain curve and the force vs. displacement curve are presented later based on the obtained data.

Fig. 8 shows the flexural stress vs. strain curve, where maximum stress was found to correspond with strain. The maximum stress (81.76 MPa) for the 3 % RHA + JF was observed to be the highest among the seven samples. Subsequently, the composite sample of 2 % RHA + JF sample (69.89 MPa), 1 % RHA + JF sample (68.99 MPa), 0 % RHA + JF sample (65.91 MPa), while the 0 % RHA + CF sample (38.18 MPa), 1 % RHA + CF sample (35.25 MPa), and lastly the 3 % RHA + CF sample (31.61 MPa) exhibit the lowest maximum stress value. With the increase in the RHA percentage, the workability decreases significantly. A similar trend was observed in the study by

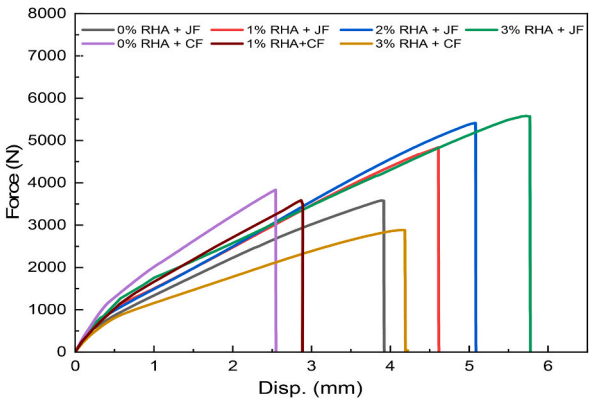

Fig. 6. Tensile test force vs. displacement curve.

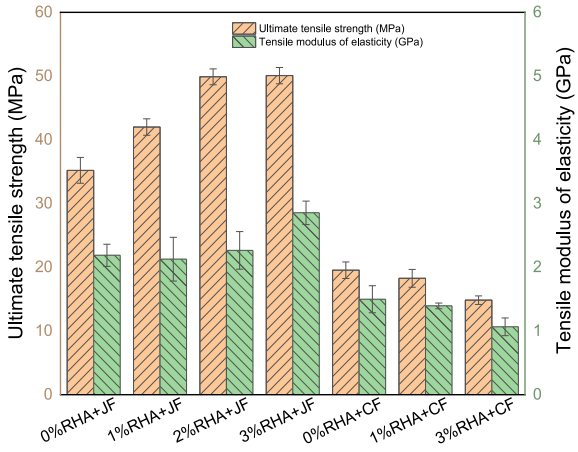

Fig. 7. Tensile test results comparison of all composites.

Table 4
Flexural test results.

SL	Specimen Name	Ultimate Force (N)	Flexural Modulus of Elasticity (GPa)	Ultimate Flexural Strength (MPa)	Energy Absorption (J)
1	0 % RHA + JF	252.537	3.095	65.9144	1.0648
		192.648	2.789	64.8447	0.8846
		253.653	2.673	65.1352	2.2989
2	1 % RHA + JF	236.691	2.933	65.7794	0.7635
		260.652	2.636	68.9895	1.0467
		262.206	2.313	65.2803	1.1435
3	2 % RHA + JF	262.361	2.507	65.6115	0.8238
		250.491	2.488	69.8995	1.1233
		277.961	2.162	68.5656	1.0861
4	3 % RHA + JF	322.35	2.948	81.7589	1.7376
		313.584	2.578	76.7727	1.9304
		312.396	2.354	73.7439	2.5001
5	0 % RHA + CF	188.715	2.309	38.1871	0.4214
		196.581	2.185	34.3269	0.6065
		173.919	2.317	34.4887	0.5310
6	1 % RHA + CF	191.677	1.895	35.2516	1.1598
		185.365	1.845	34.5925	1.2954
		173.985	1.758	32.2532	1.5875
7	3 % RHA + CF	171.00	0.842	22.9173	2.2227
		202.974	1.014	27.7483	3.3725
		185.835	1.025	31.6127	3.3950

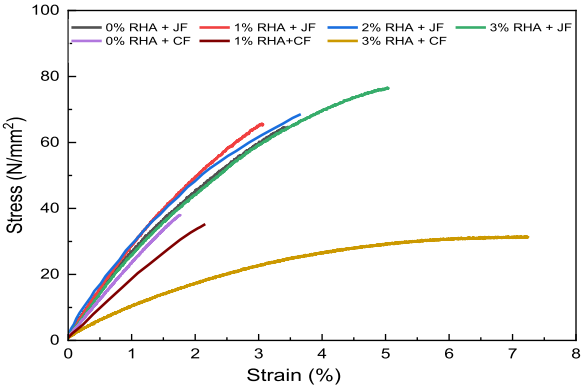

Fig. 8. Flexural test stress vs. strain curve.

Tutur et al. [34], where an increase in the percentage of rice husk ash (RHA) led to a reduction in the compressive strength of the composite. This suggests that higher RHA content may compromise the material's ability to withstand compressive stresses and hardness.

Fig. 9 indicates the force vs. displacement curve of the flexural test, with a maximum force of 322.35 N, the 3 % RHA + JF sample surpasses the other seven samples considerably. The sample made up of 2 % RHA and jute fiber has the second-highest maximum force value, measuring 277.96 N. The maximum forces of 253.653 N, 262.206 N, 196.581 N, 191.677 N, and 202.974 N are the respective values for the composites with 0 % RHA + JF, 1 % RHA + JF, 0 % RHA + CF, 1 % RHA + CF, and 3 % RHA + CF, respectively.

Fig. 10 shows the seven different composite samples with considerably varying flexural properties. The 3 % RHA and jute fiber composite have the average ultimate flexural strength (77.43 MPa), followed by the 2 % RHA + JF sample (68.03 MPa), which is the second highest, the 1 % RHA + JF sample (66.65 MPa), the 0 % RHA + JF sample (65.96 MPa), while the 0 % RHA + CF sample (35.67 MPa), 1 % RHA + CF sample (34.03 MPa), and lastly the 3 % RHA + CF sample (27.43 MPa) that indicates the lowest ultimate flexural strength. In the case of the stiffest composite, it is 0 % RHA + JF, with a flexural modulus of elasticity (avg.) of 2.85 GPa. The 1 % RHA + JF and 3 % RHA + JF composites had the second-highest flexural modulus of elasticity, measuring an average of 2.63 GPa, while 2 % RHA + JF has the lowest of 2.38 GPa. This means that the 3 % RHA + JF composite is the stiffest of the seven, while the 0 % RHA + JF composite has a decent stiffness. Moreover, the flexural modulus of elasticity for CF decreases with an increase in the filler percentage as 0 % RHA + CF, 1 % RHA + CF, and 3 % RHA + CF found of 2.27, 1.84, and 0.96 GPa, respectively.

Fig. 11 shows the energy absorption both for tensile and flexural tests with varying filler percentages. In terms of tensile energy absorption, 2 % RHA and jute fiber composite have the highest value for energy absorption with an average value of 19.23J. A higher energy absorption capability implies that the composite material can absorb more energy before failure or significant damage occurs. While 3 % RHA + JF composite also exhibits a moderate value of 16.15 J. On the contrary for the flexural energy absorption, the 3 % RHA + CF composite absorbs the most energy, with a value of 3.00 J. The higher energy absorption capability indicates that the composite material can absorb more energy before failing or causing substantial damage. While 3 % RHA + JF composite has the second highest energy absorption value of 2.06 J.

3.3. Thermal properties

Fig. 12(a–d) shows the variation of surface temperatures and heat flux with respect to time for varying RHA with jute and coconut fiber. The blue line indicates the temperature difference, the grey line indicates the outer surface temperature and the red line indicates the inside surface temperature of the sample. In the right side figure, the black line indicates the heat flux of the samples. For 0 % RHA + JF, it is found from the above graph at steady state condition, the average temperature difference of the sample has been observed of 4.4544 K and the average heat flux of 46.48 W/m^2. Similarly, for the other three samples of jute fibers having 1 % RHA + JF, 2 % RHA + JF, and 3 % RHA + JF, the average temperature differences are observed as 4.6584 K, 5.3542 K, and 6.5712 K. While the average heat flux of above three samples is recorded as 46.656 W/m^2, 48.052 W/m^2, and 51.34 W/m^2, respectively. While for the 0 % RHA + CF, it is found from the above graph at steady state condition, the average temperature difference of the sample has been observed at 5.7042 K and also the average heat flux has been found at 37.124 W/m^2. Similarly, in the other samples of coconut fiber of 1 % RHA + CF and 3 % RHA + CF at steady state conditions, the average temperature differences of the samples are found of 5.3981 K, 4.7596 K, and the average heat fluxes are found as 38.273 W/m^2 and 39.982 W/m^2, respectively. After obtaining the steady-state points for the inside surface temperature of the samples (thickness, dx = 4.464 mm), the average temperature difference is calculated from the inner and outer surface temperatures and also calculated the average heat flux for the corresponding samples. Moreover, the thermal conductivity of the seven samples was found using Fourier's law of heat conduction of Eq. (8). Finally, the measured thermal conductivity of the seven samples is listed in Table 5.

Fig. 13 shows the thermal conductivity value compared with seven types of samples. The x-axis filler weight percentage and the y-axis represent thermal conductivity in W/(m. K). Comparing all of the fabricated composites, it is seen that the thermal conductivity of jute fiber reinforced epoxy composite decreases as the filler weight percentage increases, which was desirable for the purpose of this

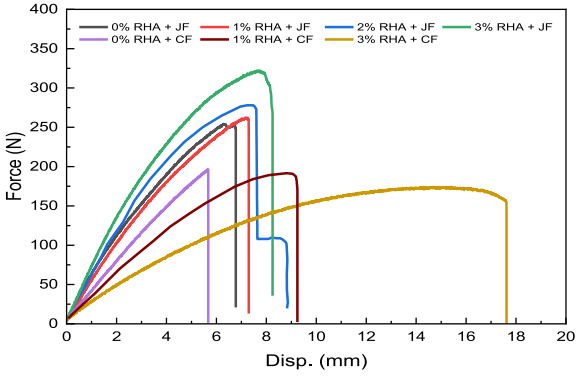

Fig. 9. Flexural test force vs. displacement curve.

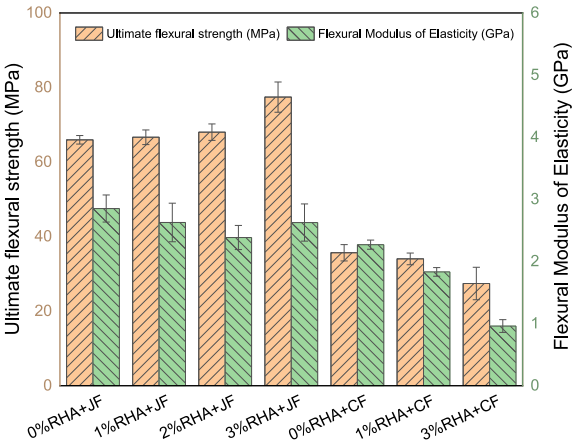

Fig. 10. Flexural test results comparison of all composites.

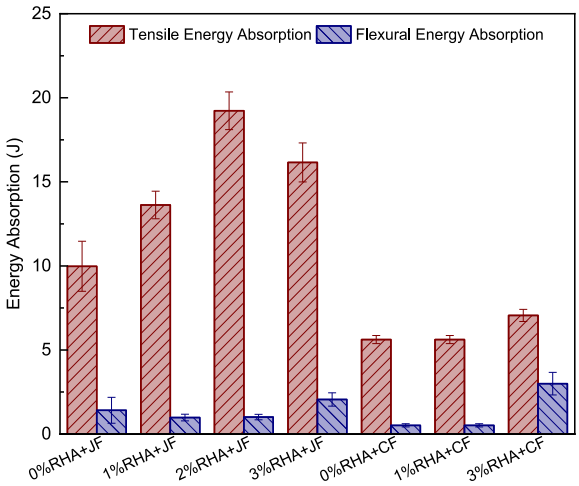

Fig. 11. Energy absorption during the tensile and flexural test with varying filler percentage.

study. RHA includes silica, which helps reduce the thermal conductivity of composite materials. The 3 % RHA + JF sample has the lowest thermal conductivity value, 0.03697 W/(m. K). In JF composites, the better dispersion of RHA and stronger bonding reduce heat conduction by creating an effective barrier to thermal pathways.

Unlike jute fiber composites, the thermal conductivity of CF composites increased with higher RHA content, peaking at 0.07469 W/m.K for the 3 % RHA + CF, while the minimum at 0.05298 W/m.K for the 0 % RHA + CF composites. The addition of filler in the coconut fiber composite increases thermal conductivity due to a variety of factors, including the relatively less porous behavior of CF, and the dispersion of fillers within the composites. Additionally, the inherently lower thermal conductivity of jute fibers compared to coconut fibers enhances the insulating performance of JF composites, making them more suitable for thermal insulation.

3.4. Heat transfer through the building wall

In this study, two types of composite walls are considered for solving the problem analytically to estimate the heat flow through the walls for the purposes of building insulation. The first one is a three-layer composite wall (type 1) consisting of two outside layers of typical concrete and an insulating prepared composite in the middle, while the other is a two-layer composite wall (type 2) consisting of the outside layer built of typical concrete and the inner layer is prepared composite as an insulating material, as illustrated in Fig. 14 (a) and (b), respectively.

For type 1, the total heat flow through a three-layer composite wall can be calculated using the following Eq. (10):

$$T_1 - T_4 = Q_1\left[\frac{x_8}{k_8 A} + \frac{x_i}{k_i A} + \frac{x_9}{k_9 A}\right] \tag{10}$$

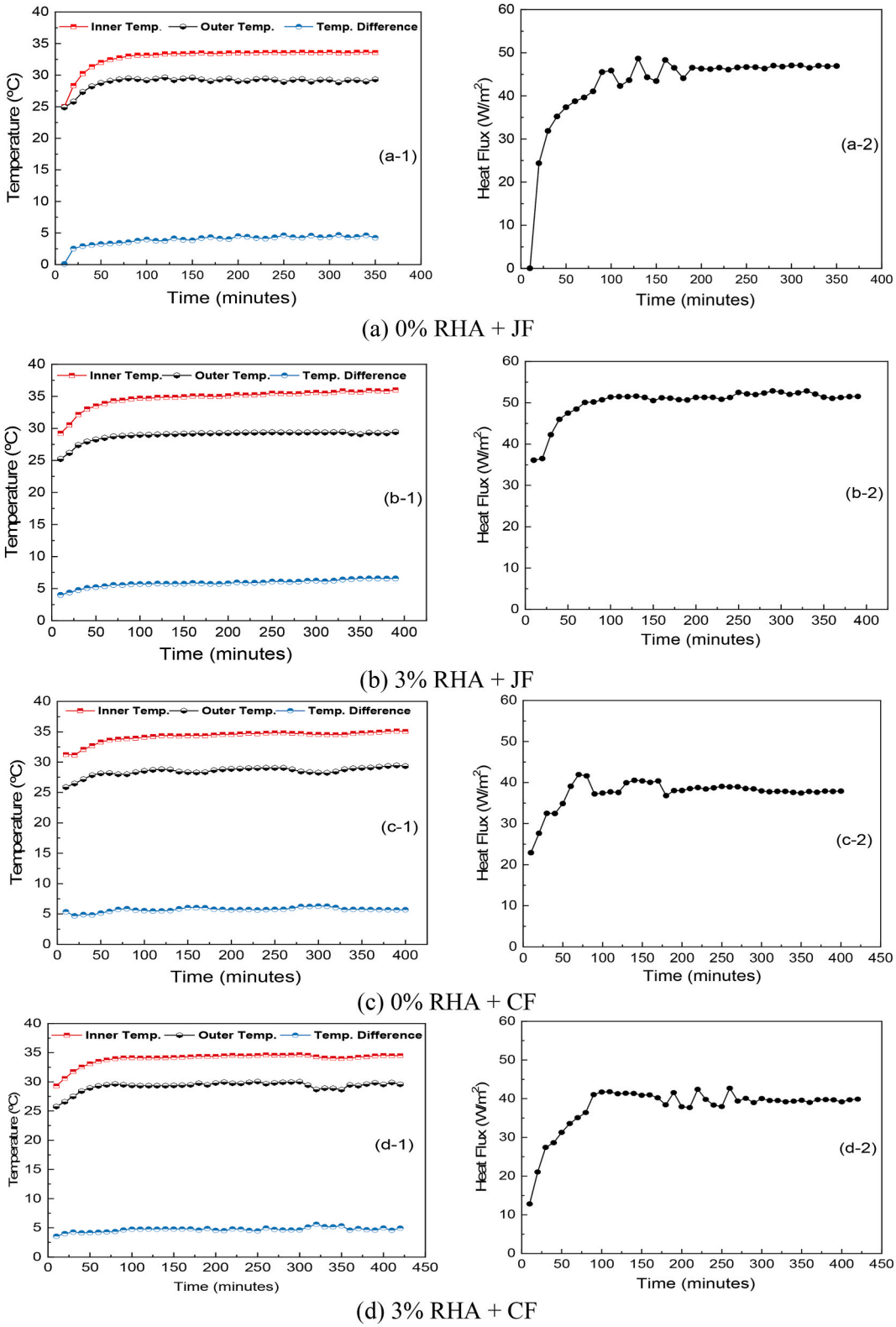

Fig. 12. Variation of surface temperatures and heat flux with time for (a) 0 % RHA + JF, (b) 3 % RHA + JF, (c) 0 % RHA + CF, and (d) 3 % RHA + CF.

Table 5
Thermal conductivity results.

SL No.	Specimen	Avg. thickness, x_i (mm)	Avg. heat flux, q (W/m^2)	Temp. difference, dT (K)	Thermal conductivity, k (W/mK)
1	0%RHA + JF	4.464	46.48	4.4544	0.04658
2	1%RHA + JF	4.3875	46.656	4.6584	0.04394
3	2%RHA + JF	4.2308	48.052	5.3542	0.03797
4	3%RHA + JF	4.7316	51.34	6.5712	0.03697
5	0%RHA + CF	8.1375	37.124	5.7024	0.05298
6	1%RHA + CF	8.3865	38.273	5.3981	0.06122
7	3%RHA + CF	8.8916	39.982	4.7596	0.07469

*Avg. means "Average", and Temp. means "Temperature".

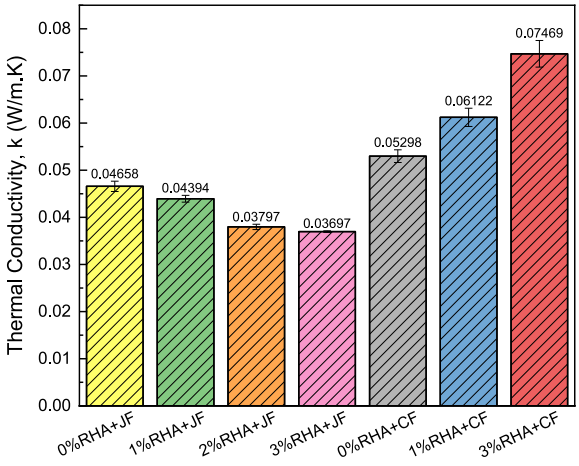

Fig. 13. Comparison of thermal conductivity.

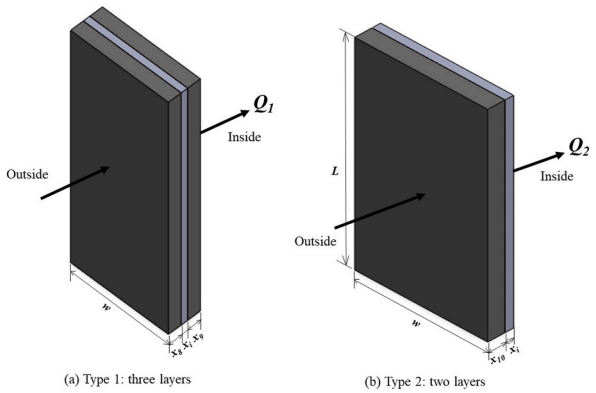

Fig. 14. Illustration for heat flow through a composite wall: (a) three layers, and (b) two layers.

Again for type 2, the total heat flow through a two-layer composite wall can be calculated using the following Eq. (11):

$$T_1 - T_4 = Q_2\left[\frac{x_{10}}{k_{10}A} + \frac{x_i}{k_iA}\right] \tag{11}$$

Where, Q_1 and Q_2 are the rate of heat transfer through the wall material (W), k_i ($i = 1, 2, 3, 4, 5, 6,$ and 7), k_8, k_9, and k_{10} are the thermal conductivity of the materials (W/m.K), A is the cross-sectional area through which heat is flowing (m^2), x_i ($i = 1, 2, 3, 4, 5, 6,$ and 7), x_8, x_9, and x_{10} are the thickness of each layer of the composite wall (m), and T_1 & T_4 are the outer and inner surface temperature of the composite wall (°C).

As the heat transfer analysis was conducted analytically, the following considerations are taken into account for the solution of the building's wall insulation. The total thickness of the composite wall is 254 mm (10 inches). The thermal conductivity (k_i) of fabricated

seven specimens was measured using the TRSYS01 measurement unit which has been listed in Table 5 and also illustrated in Fig. 13, while the thickness (x_i) is recorded for calculated the heat transfer analytically through the composite wall (taking, i = 1, 2, 3, 4, 5, 6, and 7). By the way, the considerations for analyzing the analytical solution of heat transfer of the composites for the type 1 and type 2 walls are listed as following Table 6:

For measuring the heat transfer through the composite wall, the analytical solution is to be carried out while two cases (type 1 and type 2) of study are done. To ensure optimal thermal comfort within a building, the interior temperature should be maintained between 21 and 22 °C. Considering the area of the composite wall ($A = 3 \times 6 = 18\ m^2$), while for the proper thermal comfort inside the room inner temperature, $T_4 = 22$ °C. In summer, the input temperature is considered one time at maximum temperature ($T_1 = 45$ °C) and another time at minimum temperature ($T_1 = 27.5$ °C) shown in Table 7. However, the information listed in Table 7 shows how temperatures vary by season in South Asian countries [72]. In this study, it has been performed analytically to maintain the comfort of room inside temperature (22 °C) both in summer and winter. Furthermore, for winter the average maximum ($T_1 = 17.5$ °C) & minimum ($T_1 = 7.5$ °C) temperatures are considered. Similarly, the total heat transfer for different insulating materials can be calculated for variations of seasons. The heat transfer of type 1 and type 2 composite walls was obtained as listed in Tables 8 and 9, respectively. Meanwhile, the negative sign indicates the reverse direction of heat flow. It is found that the heat transfer of composite walls of type 1 and type 2 are observed as almost similar trends of findings.

Moreover, Fig. 15 shows the bar chart indicating the heat transfer through the composite wall for summer and winter seasons according to maximum & minimum temperature (at 45 °C & 27.5 °C for summer and at 17.5 °C & 7.5 °C for winter). It is found that the obtained heat transfer through the composite wall (type 1 and type 2) is decreased when the filler used increases to 0–3 % of RHA with jute fiber and coconut fiber composites. As the heat transfer rate through composite walls of type 1 and type 2 is almost similar, it is suggested to use the type 2 wall insulation in actual practice due to easily fabricate/attach the insulating material as prepared specimen into the inner surface of the building wall than the middle of insulating material as prepared specimen between two concrete layers.

4. Comparison with traditional insulation materials

4.1. Insulation efficiency

From this study, the 3 % RHA + JF composite shows the lowest thermal conductivity of 0.03697 W/m.K and for this reason, it is suggested for the building thermal insulation. From the literature, foam plastics are widely used as the most traditional materials for building thermal insulation while two types are expanded polystyrene (EPS) and polyurethane foam (PU). The thermal conductivity of EPS is in the range of 0.035–0.040 W/m·K [73,74], while the PU is in the range of 0.035–0.045 W/m·K [75]. However, Fig. 16 shows the comparison of the thermal conductivity of the 3 % RHA + JF composite with EPS Foam and PU Foam plastics. The 3 % RHA + JF composite shows a thermal conductivity of 0.03697 W/m·K, which is comparable to or even better than common insulation materials like EPS and PU foams, which typically range between 0.035 and 0.045 W/m·K. It is concluded that the 3 % RHA + JF composite offers comparable thermal insulation to conventional foam plastics (EPS and PU foam), making it a viable alternative for thermal insulation in buildings.

4.2. Cost analysis and environmental impact

In terms of processing, the hand lay-up method was used which is simple and cost-effective for small-scale production. However, for industrial-scale manufacturing, more automated processes, such as compression molding or resin transfer molding, may be needed. These methods could increase production efficiency but may also raise processing costs. Even yet, Jute-RHA composites are expected to be cheaper than traditional foam materials due to the environmental benefits of using waste materials like RHA and the lesser energy needed to manufacture natural fibers like jute. However, this analysis evaluates the cost of producing a 3 % RHA + JF sample and compares its cost per square meter with EPS and PU foam plastics.

The cost of producing a 300 × 300 mm (0.09 m^2) sample of the 3 % RHA + JF composite is approximately 355.72 BDT per sample, or 3952.44 BDT per square meter (m^2), which is roughly 34.38 USD/m^2. This cost is higher due to the small-scale production for testing purposes. However, if the composite were produced in bulk for large-scale insulation applications, the cost could be reduced by up to 50 % [76]. The 3 % JF + RHA composite, with a bulk production cost of 17.18 USD/m^2, is highly competitive when compared to PU foam (21.74 USD/m^2) and EPS foam (8.7 USD/m^2). While its price is closer to PU foam, the composite offers significant advantages that make it a standout choice for insulation. The details of cost estimation are listed in Table 10.

JF + RHA composite is a renewable and biodegradable material, while the PU and EPS foams are non-biodegradable and contribute significantly to plastic pollution, often ending up in landfills or oceans, where they persist for hundreds of years [79]. The production

Table 6
Considerations are taken into account for the solution of building wall insulation.

Composite wall	Thermal conductivity (W/m.K)		Thickness (mm)	
Type 1	$k_8 = k_9$	k_i	$x_8 = x_9$	x_i
	0.5	listed in Table 5	125	listed in Table 5
Type 2	k_{10}	k_i	x_{10}	x_i
	0.5	listed in Table 5	250	listed in Table 5

Table 7
Maximum & minimum temperature according to seasons [72].

Seasons	Temperature (°C)	
	Maximum	Minimum
Summer	40–50	25–30
Winter	15–20	5–10

Table 8
Heat transfer for type 1 composite wall.

Insulating materials	Heat transfer through the composite wall, Q (W)			
	For summer		For winter	
	At maximum temperature	At minimum temperature	At maximum temperature	At minimum temperature
0 % RHA + JF	706.93	169.19	−138.87	−444.89
1 % RHA + JF	700.89	167.85	−137.93	−441.86
2 % RHA + JF	684.09	163.87	−134.18	−431.83
3 % RHA + JF	681.02	162.98	−133.78	−429.14
0 % RHA + CF	719.89	172.32	−140.17	−454.65
1 % RHA + CF	729.27	174.87	−141.13	−459.57
3 % RHA + CF	748.17	179.13	−146.83	−472.05

Table 9
Heat transfer for type 2 composite wall.

Insulating materials	Heat transfer through the composite wall, Q (W)			
	For summer		For winter	
	At maximum temperature	At minimum temperature	At maximum temperature	At minimum temperature
0 % RHA + JF	706.64	168.98	−138.25	−445.49
1 % RHA + JF	700.47	167.50	−137.05	−441.60
2 % RHA + JF	683.90	163.54	−133.81	−431.16
3 % RHA + JF	680.70	162.77	−133.18	−429.14
0 % RHA + CF	719.37	172.02	−140.75	−453.52
1 % RHA + CF	728.98	174.52	−141.59	−458.85
3 % RHA + CF	747.90	178.84	−146.33	−471.50

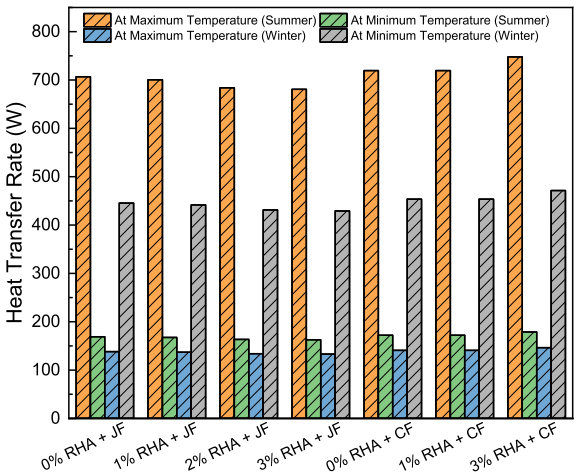

Fig. 15. Heat transfer through the composite wall for summer and winter seasons according to maximum & minimum temperature.

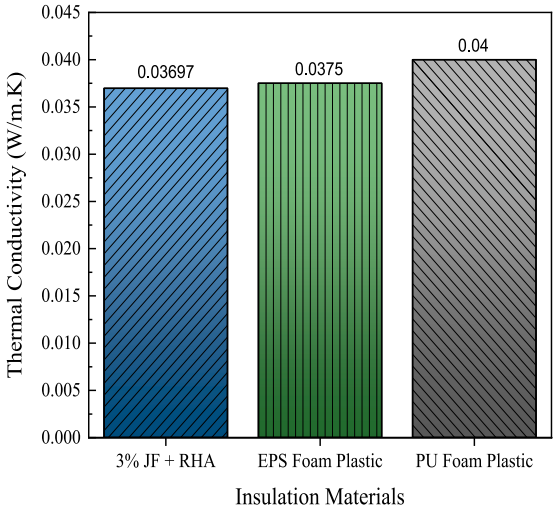

Fig. 16. Comparison of the thermal conductivity with traditional insulation materials: EPS foam [73,74] and PU foam [75] plastics.

Table 10
Cost comparison of JF + RHA over traditional materials.

Material	Cost (BDT/m^2)	Cost (USD/m^2)
3 % JF + RHA Composite (Limited)	3952.44	34.38
3 % JF + RHA Composite (Bulk, 50 % Reduction)	1976.22	17.18
EPS Foam [77]	1000.00	8.7
PU Foam [78]	2500.00	21.74

process of both PU and EPS foams is highly energy-intensive. PU foam, for instance, consumes approximately 4–8 kWh of electricity per kilogram during production. This means that producing a cubic meter of PU foam, which weighs around 35–50 kg, could consume 140–400 kWh of electricity [80]. EPS foam, while slightly less energy-consuming, still requires about 2–4 kWh per kilogram, amounting to 40–160 kWh per cubic meter of foam. In comparison, the 3 % JF + RHA composite uses natural materials and a simpler production process, resulting in much lower energy consumption and a smaller overall carbon footprint. In addition to its thermal efficiency, the composite's biodegradability and lower environmental impact make it a far superior alternative to both PU and EPS foams, which are produced using toxic chemicals and emitting harmful gases like HCFCs and HFCs. While the 3 % JF + RHA composite may be priced similarly to PU foam, its eco-friendly properties and reduced environmental impact make it an ideal choice for those seeking sustainable and high-performance building insulation.

5. Conclusion

In this study, the investigation of the suitability of epoxy composites reinforced with coconut and jute fibers for thermal insulation applications in buildings was done where the composites were prepared using the hand lay-up method with varying percentages of RHA filler. The specific findings of this research are as follows:

- The tensile values improve with increasing filler percentage in the jute fiber composites while decreasing strength with increasing filler percentage in coconut fiber composites. It is observed that the 3 % RHA and jute fiber composite with ultimate tensile strength of 50.07 MPa and highest tensile modulus of elasticity, and good energy absorption. This indicates that the 3 % RHA and jute fiber composite is the best material of the seven specimens in terms of strength, stiffness, and energy absorption making it an excellent choice for structural applications. Meanwhile, the 3 % RHA + coconut fiber composite is the weakest.
- The flexural properties decrease with increasing filler percentage in the coconut fiber composites, while the 3 % RHA and jute fiber composite show the highest ultimate flexural strength and moderate flexural modulus of elasticity. The results show that, in terms of strength, stiffness, and energy absorption, the 3 % RHA + Jute Fiber composite performs overall the best out of the seven materials, making it a great option for building purposes.
- The thermal conductivity is decreased with increasing filler weight percentage in jute fiber composites, on the contrary, it is increased with increasing filler weight percentage in CF composites. The minimum thermal conductivity is observed as 0.03697 W/m.K in 3 % RHA + JF composite.

- The study concluded that the 3 % RHA + JF composite sample has the lowest thermal conductivity, good strength, and reasonable stiffness and energy absorption capacity, making it suitable for improving thermal insulation in buildings.
- The obtained heat transfer through the composite wall (type 1 and type 2) is decreased when the filler used increases as 0–3 % of RHA with jute fiber and coconut fiber composites. As the heat transfer rate through composite walls of type 1 and type 2 is almost similar heat transfer rate, it is suggested to use the type 2 composite in actual practice due to easily fabricate the insulating material as prepared specimen into the inner surface of the building wall than the middle of insulating material as prepared specimen between two concrete layers.

The scope of exploring jute and coconut fiber-reinforced epoxy composites with rice husk ash filler for building insulation is promising. These sustainable composites, made from agricultural waste, align with green building practices and can reduce environmental impact. They offer improved thermal insulation, leading to energy-efficient buildings and lower greenhouse gas emissions. Their lightweight nature simplifies transportation and installation, cutting costs and time. Their versatility in various building components and potential for improved properties through ongoing research further boost their viability as a sustainable construction material.

CRediT authorship contribution statement

Md. Ahtesham Akhter: Writing – review & editing, Writing – original draft, Visualization, Methodology, Investigation, Data curation, Conceptualization. **Dipayan Mondal:** Writing – review & editing, Writing – original draft, Visualization, Validation, Supervision, Resources, Methodology, Investigation, Formal analysis, Data curation, Conceptualization. **Arup Kumar Debnath:** Writing – review & editing, Writing – original draft, Visualization, Formal analysis, Data curation. **Md. Ashraful Islam:** Writing – review & editing, Writing – original draft, Visualization, Formal analysis, Data curation. **Md. Sanaul Rabbi:** Writing – review & editing, Writing – original draft, Visualization, Data curation.

Data and code availability statement

Data will be available from the corresponding author upon reasonable request. Moreover, no code was used for the research described in the article.

Funding statement

This research did not receive any specific grant from funding agencies in the public, commercial, or not-for-profit sectors.

Declaration of competing interest

The authors declare that they have no known competing financial interests or personal relationships that could have appeared to influence the work reported in this paper.

Acknowledgment

The authors appreciate and acknowledge the Khulna University of Engineering & Technology for providing the facilities throughout this work.

References

[1] A.P. Wibowo, M. Saidani, M. Khorami, M. Bai, The Heat Transfer Rate of Composite Wall with Series and Parallel Configuration, 2022.
[2] Y.K. Sahu, Study on the Effective Thermal Conductivity of Fiber Reinforced Epoxy Composites, 2014.
[3] H. Ahmad, M.A. Islam, M.F. Uddin, Thermal and Mechanical Properties of Epoxy-Jute Fiber Composite, 2012.
[4] S. Biswas, S. Shahinur, M. Hasan, Q. Ahsan, Physical, mechanical and thermal properties of jute and bamboo fiber reinforced unidirectional epoxy composites, Procedia Eng. 105 (2015) 933–939, https://doi.org/10.1016/j.proeng.2015.05.118.
[5] N.L. Hancox, Engineering mechanics of composite materials, Mater. Des. 2 (17) (1996) 114.
[6] J.S. Chohan, K.S. Boparai, R. Singh, M.S.J. Hashmi, Manufacturing techniques and applications of polymer matrix composites: a brief review, Adv. Mater. Process. Technol. 8 (1) (2022) 884–894, https://doi.org/10.1080/2374068X.2020.1835012.
[7] S.G. Advani, K.-T. Hsiao, Manufacturing Techniques for Polymer Matrix Composites (PMCs), Elsevier, 2012.
[8] F. Zhang, X. Wang, J.B. Wierschke, L. Wang, Helium bubble evolution in ion irradiated Al/B4C metal metrix composite, Scr. Mater. 109 (Dec. 2015) 28–33, https://doi.org/10.1016/J.SCRIPTAMAT.2015.07.011.
[9] J. Lamon, Review: creep of fibre-reinforced ceramic matrix composites, Int. Mater. Rev. 65 (1) (Jan. 2020) 28–62, https://doi.org/10.1080/09506608.2018.1564182.
[10] K. Cui, Y. Zhang, T. Fu, J. Wang, X. Zhang, Toughening mechanism of mullite matrix composites: a review, Coatings 2020 10 (7) (Jul. 2020) 672, https://doi.org/10.3390/COATINGS10070672, 10, Page 672.
[11] M. Helmi Abdul Kudus, M.M. Ratnam, H.M. Akil, "Factors affecting hole quality during drilling of natural fiber-reinforced composites, A comprehensive review," 40 (9–10) (Nov. 2020) 391–405, https://doi.org/10.1177/0731684420970650.
[12] H. Jariwala, P. Jain, A review on mechanical behavior of natural fiber reinforced polymer composites and its applications. https://doi.org/10.1177/0731684419828524, Feb. 2019, 38, no. 10, pp. 441–453.
[13] F.M.B. Coutinho, T.H.S. Costa, Performance of polypropylene–wood fiber composites, Polym. Test. 18 (8) (Dec. 1999) 581–587, https://doi.org/10.1016/S0142-9418(98)00056-7.

[14] G.M. Zakriya, G. Ramakrishnan, Insulation and mechanical properties of jute and hollow conjugated polyester reinforced nonwoven composite, Energy Build. 158 (Jan. 2018) 1544–1552, https://doi.org/10.1016/j.enbuild.2017.11.010.

[15] B.A. Praveena, A. Buradi, N. Santhosh, V.K. Vasu, J. Hatgundi, D. Huliya, Study on characterization of mechanical, thermal properties, machinability and biodegradability of natural fiber reinforced polymer composites and its Applications, recent developments and future potentials: a comprehensive review, Mater. Today: Proc. 52 (2022) 1255–1259, https://doi.org/10.1016/j.matpr.2021.11.049.

[16] D. Sarukasan, K. Thirumavalavan, M. Prahadeeswaran, R. Muruganandhan, Fabrication and mechanical characterization of jute-coir reinforced unsaturated polyester resin hybrid composites with various fiber size using compression moulding technique, Int. J. Recent Technol. Eng. 10 (1) (May 2021) 233–241, https://doi.org/10.35940/ijrte.a5934.0510121.

[17] I. Florea, D.L. Manea, Analysis of thermal insulation building materials based on natural fibers, Procedia Manuf. 32 (2019) 230–235, https://doi.org/10.1016/j.promfg.2019.02.207.

[18] I.F. Ghazi, R.I. Jaddan, Thermal conductivity characterization of epoxy based composites reinforced with date palm waste particles, J. Phys. Conf. 1973 (1) (Aug. 2021), https://doi.org/10.1088/1742-6596/1973/1/012144.

[19] S.P. Jani, S. Sajith, C. Rajaganapathy, M.A. Khan, Mechanical and thermal insulation properties of surface-modified Agave Americana/carbon fibre hybrid reinforced epoxy composites, Mater. Today: Proc. 37 (Part 2) (2020) 1648–1653, https://doi.org/10.1016/j.matpr.2020.07.180.

[20] M. Boopalan, M. Niranjanaa, M.J. Umapathy, Study on the mechanical properties and thermal properties of jute and banana fiber reinforced epoxy hybrid composites, Compos. Part B Eng. 51 (Aug. 2013) 54–57, https://doi.org/10.1016/j.compositesb.2013.02.033.

[21] R. Bhoopathi, M. Ramesh, C. Deepa, Fabrication and property evaluation of banana-hemp-glass fiber reinforced composites, Procedia Eng. 97 (Jan. 2014) 2032–2041, https://doi.org/10.1016/J.PROENG.2014.12.446.

[22] G.R. Arpitha, N. Jain, A. Verma, Banana biofiber and glass fiber reinforced hybrid composite for lightweight structural applications: mechanical, thermal, and microstructural characterization, Biomass Convers. Biorefinery (2023), https://doi.org/10.1007/S13399-023-04300-Y.

[23] M.N. Jahir, R. Mustak, A.K. Debnath, P.D. Nath, Orientation effect of jute-glass fiber reinforced composite on mechanical properties, in: Proceedings of the International Conference on Mechanical Engineering and Renewable Energy, Chattogram, Bangladesh, 2021.

[24] A.K. Debnath, R. Mustak, M.A. Hasib, Investigation of mechanical properties of timber beam reinforced with glass fiber, J. Eng. Technol. 16 (1) (2024) 1–6.

[25] M. H, et al., Effect of bio-fibers and inorganic fillers reinforcement on mechanical and thermal characteristics on carbon-kevlar-basalt-innegra fiber bio/synthetic epoxy hybrid composites, J. Mater. Res. Technol. 23 (Mar. 2023) 5440–5458, https://doi.org/10.1016/J.JMRT.2023.02.162.

[26] H.M. Kavya, S. Bavan, B. Yogesha, M.R. Sanjay, S. Siengchin, S. Gorbatyuk, Effect of coir fiber and inorganic filler on physical and mechanical properties of epoxy based hybrid composites, Polym. Compos. 42 (8) (Aug. 2021) 3911–3921, https://doi.org/10.1002/PC.26103.

[27] A. Rahman, M.A. Hasib, M.A. Islam, I. Alam, S. Chanda, Fabrication and performance investigation of natural-glass fiber hybrid laminated composites at different stacking orientations, J. Nat. Fibers 20 (1) (Apr. 2023), https://doi.org/10.1080/15440478.2022.2143981.

[28] D.S. Mondloe, et al., Investigation of mechanical and wear properties of novel hybrid composite based on BANANA, COIR, and EPOXY for tribological applications, Int. J. Eng. Trends Technol. 70 (4) (Apr. 2022) 278–285, https://doi.org/10.14445/22315381/IJETT-V70I4P224.

[29] V.V. Arun Sankar, P. Suresh, V. Arun Kumar, S. Dhanasekar, E. Harissh Kumar, R. Nandhakumar, Experimental research into the mechanical behaviour of banana fibre reinforced PP composite material, Mater. Today: Proc. 33 (2020) 3097–3101, https://doi.org/10.1016/j.matpr.2020.03.685.

[30] A.J. Hameed, S. Prasanth, T. Suseela, Hardness and flexural strength of rice husk and rice husk ash on coconut fiber reinforced polyester composites, Int. J. Emerg. Technol. Eng. Res. 5 (4) (2017) 310–313.

[31] S.M.K.S. Turjo, M.F. Hossain, M.S. Rana, M.S. Ferdous, Mechanical characterization and corrosive impacts of natural fiber reinforced composites: an experimental and numerical approach, Polym. Test. 125 (Aug. 2023) 108108, https://doi.org/10.1016/J.POLYMERTESTING.2023.108108.

[32] P. Madhu, K.N. Bharath, M.R. Sanjay, G.R. Arpitha, D. Saravanabavan, Effect of nano fillers on glass/silk fibers based reinforced polymer composites, Mater. Today Proc. 46 (18) (Jan. 2021) 9032–9035, https://doi.org/10.1016/J.MATPR.2021.05.383.

[33] F. Chen, Study on mechanical and thermal performance of building energy-saving wall with insulation materials, E3S Web of Conferences 242 (Mar. 2021), https://doi.org/10.1051/e3sconf/202124202005.

[34] N. Tutur, R.N.H.R.M. Noor, The potential of rice husk ash (Rha) and coconut fiber (Cf) as partial replacement of cement, AIP Conf. Proc. 2020 (1) (2018) 20061, https://doi.org/10.1063/1.5062687, 1–6.

[35] M.F. Omar, M.A.H. Abdullah, N.A. Rashid, A.L.A. Rani, N.A. Illias, The application of coconut fiber as insulation ceiling board in building construction, IOP Conf. Ser. Mater. Sci. Eng. 864 (1) (2020) 012196, https://doi.org/10.1088/1757-899X/864/1/012196.

[36] K.M.F. Hasan, P.G. Horváth, Z. Kóczán, D.H.H.A. Le, M. Bak, L. Bejó, T. Alpár, Novel insulation panels development from multilayered coir short and long fiber reinforced phenol formaldehyde polymeric biocomposites, J. Polym. Res. 28 (12) (2021) 467, https://doi.org/10.1007/s10965-021-02818-1, 1–16.

[37] J. Veeraprabahar, G. Mohankumar, S. Senthil Kumar, S. Sakthivel, Development of natural coir/jute fibers hybrid composite materials for automotive thermal insulation applications, J. Eng. Fiber. Fabr. 17 (2022) 1–11, https://doi.org/10.1177/15589250221136379.

[38] R.P. Patil, A. Patil, V. Hpatil, P.A. Koli, P. Student, Analysis of steady state heat conduction in different composite wall, Int. J. Innov. Res. Sci. Eng. Technol. (An ISO 3297 (2007), https://doi.org/10.15680/IJIRSET.2015.0407076.

[39] K. Ahmada, M.A. Nazira, A.K. Qureshi, E. Hussain, T. Najam, M.S. Javed, S.S.A. Shah, M.K. Tufail, S. Hussain, N.A. Khan, H.U.R. Shah, M. Ashfaq, Engineering of Zirconium based metal-organic frameworks (Zr-MOFs) as efficient adsorbents, Mater. Sci. Eng. B 262 (2020) 114766, https://doi.org/10.1016/j.mseb.2020.114766.

[40] K. Naseem, M. Arif, A.A. Haral, M.H. Tahir, A. Khurshid, K. Ahmed, H. Majeed, S. Haider, S.U.D. Khan, M.F. Nazar, A. Aziz, Enzymes encapsulated smart polymer micro assemblies and their tuned multi-functionalities: a critical review, Int. J. Polym. Mater. Polym. Biomater. 73 (9) (2023) 785–816, https://doi.org/10.1080/00914037.2023.2213379.

[41] M.V. Ch, A. Kaur, L. Vasudha, Exploitation of rice husk and ash: a review, Pharma Innov. J. 12 (3) (2023) 5203–5208 [Online]. Available: https://www.researchgate.net/publication/372109306.

[42] N.C. Amulah, A.M. El-Jummah, A.A. Hammajam, U. Ibrahim, Experimental investigation on the thermal properties of gypsum plaster-rice husk ash composite, Open J. Compos. Mater. 12 (4) (2022) 131–138, https://doi.org/10.4236/ojcm.2022.124010.

[43] F. I. Park, P. Street, and L. District, "Technical Information Little Sparrow," pp. 1–2.

[44] H. Wang, H. Memon, E.A.M. Hassan, M.S. Miah, M.A. Ali, Effect of jute fiber modification on mechanical properties of jute fiber composite, Materials 12 (8) (2019) 1226, https://doi.org/10.3390/ma12081226.

[45] M.M. Younus, N. Gayathri, Experimental study of hybrid fibre (polypropy line fibre & coconut fibre) reinforced concrete, Int. J. Innov. Sci. Res. Technol. 3 (9) (2018) 431–434.

[46] S.N. Monteiro, L.A.H. Terrones, J.R.M. D'Almeida, Mechanical performance of coir fiber/polyester composites, Polym. Test. 27 (5) (2008) 591–595, https://doi.org/10.1016/j.polymertesting.2008.03.003.

[47] E. Aprianti S, A Huge Number of Artificial Waste Material Can Be Supplementary Cementitious Material (SCM) for Concrete Production – a Review Part II, vol. 142, Elsevier Ltd, 2017, https://doi.org/10.1016/j.jclepro.2015.12.115.

[48] I. Ali, E. Ahmad, An experimental investigation on partial replacement of cement with rice husk ash and fine aggregate with steel slag, Int. J. Eng. Res. V9 (8) (2020) 725–729, https://doi.org/10.17577/ijertv9is080285.

[49] A.A. Raheem, K.O. Oriola, M.A. Kareem, R. Abdulwahab, Investigation on thermal properties of rice husk ash-blended palm kernel shell concrete, Environ. Challenges 5 (July) (2021) 100284, https://doi.org/10.1016/j.envc.2021.100284.

[50] M. Bilal, Composite Formation by hand lay-up process, Reg. No. 12-3-1-022 (2022).

[51] D. D3039/D3039M−14, Standard Test Method for Tensile Properties of Polymer Matrix Composite Materials, vol. 1, 2017, https://doi.org/10.1520/D3039_D3039M-14.

[52] Shimadzu, Precision universal testing machines AUTOGRAPH AGX-V series. https://www.shimadzu.com/an/sites/shimadzu.com.an/files/pim/pim_document_file/brochures/17011/c224-e122.pdf, 2019.

[53] A. International and files indexed by mero, "Designation: D 3039/D 3039M-00 e1 Standard Test Method for Tensile Properties of Polymer Matrix Composite Materials vol. 1".
[54] D. D7264/D7264M−07, Standard Test Method for Flexural Properties of Polymer Matrix Composite Materials, vol. 1, 2015, https://doi.org/10.1520/D7264_D7264M-07.
[55] C. Zweben, W.S. Smith, M.W. Wardle, Test Methods for Fiber Tensile Strength, Composite Flexural IVIodulus, and Properties of Fabric-Reinforced Lanninates, STP 674, ASTM Spec. Tech. Publ., 1979, pp. 228–262, https://doi.org/10.1520/STP36912S.
[56] Hukseflux, Hukseflux Thermal Sensors - user Manual HF05, High-accuracy building thermal resistance measuring system with two measurement locations. https://www.hukseflux.com/uploads/product-documents/HF05_manual_v2126.pdf, 2021.
[57] I.S. Liu, On Fourier's law of heat conduction, Contin. Mech. Thermodyn. 2 (4) (Dec. 1990) 301–305, https://doi.org/10.1007/BF01129123.
[58] P. Karua, M. Arifuzzaman, M.S. Islam, Effect of jute fiber reinforcement on the mechanical properties of expanded perlite particles-filled gypsum composites, Constr. Build. Mater. 387 (April) (2023) 131625, https://doi.org/10.1016/j.conbuildmat.2023.131625.
[59] F.M. Saif, M.S. Islam, Investigation of mechanical properties of bagasse fiber and human hair reinforced hybrid composite, in: Proceedings of the International Conference on Mechanical, Industrial and Energy Engineering, 2020. Khulna, Bangladesh.
[60] F. Hossain, M. Arifuzzaman, M.S. Islam, M.M. Islam, Thermo-mechanical behavior of green sandwich structures for building and construction applications, Processes 11 (8) (2023), https://doi.org/10.3390/pr11082456.
[61] M.J. Hossain, Experimental and Numerical Investigation on Thermal Performance of Building Envelopes under Climate in Bangladesh, Department of Energy Science Engineering, Khulna University of Engineering & Technology, Khulna, Bangladesh, 2023. M.Sc. Thesis.
[62] JCGM 100, Evaluation of Measurement Data-Guide to the Expression of Uncertainty in Measurement, GUM 1995 with Minor Corrections, 2008.
[63] B.N. Taylor, C.E. Kuyatt, Guidelines for Evaluating and Expressing the Uncertainty of NIST Measurement Results, 1994.
[64] S. Bell, "A beginner's guide to uncertainty of measurement, Measurement Good Practice Guide No. 11 (Issue 2) (2001). Teddington, Middlesex, United Kingdom, TW11 0LW.
[65] W. Gabauer, Manual of codes of practice for the determination of uncertainties in mechanical tests on metallic materials, code of practice No. 07: the determination of uncertainties in tensile testing, VOEST-ALPINE STAHL LINZ GmbH Voest-Alpine, Voest-Alpine Straße, 3 4031 Linz, AUSTRIA Issue (1) (2000) 33.
[66] A. Shamsuri, M. Awing, M. Tawil, Calculation of measurement uncertainty for tensile strength and flexural strength of thermoplastic, Asian Res. J. Math 1 (3) (2016) 1–11, https://doi.org/10.9734/arjom/2016/28947.
[67] D. Mondal, A.R. Tuhin, K. Kariya, A. Miyara, Measurement of kinematic viscosity and thermal conductivity of 3,3,4,4,5,5-HFCPE in liquid and vapor phases, Int. J. Refrig. 140 (May) (2022) 150–165, https://doi.org/10.1016/j.ijrefrig.2022.05.002.
[68] D. Mondal, K. Kariya, A.R. Tuhin, N. Amakusa, A. Miyara, Viscosity measurement for trans-1,1,1,4,4,4-hexafluoro-2-butene(R1336mzz(E)) in liquid and vapor phases, Int. J. Refrig. 133 (2022) 267–275, https://doi.org/10.1016/j.ijrefrig.2021.10.006. October 2021.
[69] D. Mondal, K. Kariya, A.R. Tuhin, K. Miyoshi, A. Miyara, Thermal conductivity measurement and correlation at saturation condition of HFO refrigerant trans-1,1,1,4,4,4-hexafluoro-2-butene (R1336mzz(E)), Int. J. Refrig. 129 (2021) 109–117, https://doi.org/10.1016/j.ijrefrig.2021.05.005.
[70] D. Mondal, Y. Hori, K. Kariya, A. Miyara, M. Jahangir Alam, Measurement of viscosity of a binary mixture of R1123 + R32 refrigerant by tandem capillary tube method, Int. J. Thermophys. 41 (6) (2020) 1–20, https://doi.org/10.1007/s10765-020-02653-4.
[71] G.H.M.J.S. De Silva, P. Naveen, Effect of rice husk ash and coconut coir fiber on cement mortar: enhancing sustainability and efficiency in buildings, Constr. Build. Mater. 440 (August) (2024) 137326, https://doi.org/10.1016/j.conbuildmat.2024.137326.
[72] A. Highlight, "Plan a Travel to Southeast Asia in Summer 2024/2025." https://www.asiahighlights.com/southeast-asia/summer-trip-planner.
[73] M. Ashby, K. Johnson, Materials and design: the art and science of material selection in product design, Available: https://www.researchgate.net/publication/31726716_Materials_and_Design_The_Art_and_Science_of_Material_Selection_in_Product_Design_M_Ashby_K_Johnson. (Accessed 15 December 2024).
[74] R. R. Zarr and A. L. Pintar, Standard Reference Materials: SRM 1453, Expanded Polystyrene Board, for Thermal Conductivity from 281 K to 313 K, NIST Special Publication 260-175, doi: 10.6028/NIST.SP.260-175.
[75] T. Stovall, Closed cell foam insulation: a reviewof long term thermal performance research, ORNL/TM-2012/583, https://info.ornl.gov/sites/publications/files/Pub40530.pdf, 2012. (Accessed 15 December 2024).
[76] C. Blommaert, W. Van Paepegem, J. Degrieck, Design of composite Material for cost effective large scale production of components for floating offshore structures, Plast., Rubber Compos. 38 (2–4) (2009) 146–152, https://doi.org/10.1179/174328909X387883.
[77] EPS Insulation Cost Guide - 2024, EPS Insulation Typical Options and Example Cost Estimates for Your Area - Homewyse.com, Available: https://www.homewyse.com/costs/cost_of_eps_insulation.html (Accessed: December. 15, 2024).
[78] Spray foam insulation cost - HomeGuide. https://homeguide.com/costs/spray-foam-insulation-cost. (Accessed 15 December 2024).
[79] C.O. Adetunji, O.T. Olaniyan, O.A. Anani, A. Inobeme, J.T. Mathew, Environmental impact of polyurethane chemistry, ACS Symp. Ser. 1380 (2021) 393–411, https://doi.org/10.1021/bk-2021-1380.ch014.
[80] A. Kairytė, M. Kirpluks, A. Ivdre, U. Cabulis, S. Vaitkus, I. Pundienė, Cleaner production of polyurethane foam: replacement of conventional raw materials, assessment of fire resistance and environmental impact, J. Clean. Prod. 183 (2018) 760–771, https://doi.org/10.1016/j.jclepro.2018.02.164.